Timber shear walls with large openings: experimental and numerical prediction of the structural behaviour

Nicolas Richard, Laurent Daudeville, Helmut Prion, and Frank Lam

Abstract: A numerical model based on the finite element method is presented for prediction of the cyclic response of wood frame structures. The model predicts the cyclic response of shear walls. Nonlinear phenomena are assumed to be concentrated in the connections that are modelled through elements linking the structural elements including the posts, beams, and sheathing panels. Identification of model parameters relies on tests on individual connections. Connection tests on different nail lengths were conducted under monotonic and cyclic lateral loads. Based on the results from past studies that indicate the pull-through failure is an important failure mode in common nail connections with lumber and oriented strand board (OSB), washers were considered as a means to reinforce the connection. The influence of reinforced nailing on the static and dynamic performance of full-size wood frame shear walls with large openings, sheathed with OSB panels, was evaluated experimentally. Combinations of parameters were studied, such as the number of hold-downs, the panel shapes, the nail distribution, and the bracing systems. Comparisons of the dissipated energy per cycle revealed a higher capacity for walls using nails with washer reinforcement than without. Results from numerical simulations of the monotonic and cyclic tests performed on the walls are presented.

Key words: timber shear wall, connections, finite element, dissipated energy.

Résumé : Une approche fondée sur la méthode des éléments finis est proposée pour la prédiction de la résistance de structures bois sous chargement monotone et cyclique. Les phénomènes de dégradation sont supposés concentrés dans les assemblages reliant les éléments structuraux. L'identification des paramètres de la méthode repose sur des essais de connections. L'étude de connections par clous lisses entre des poutres et des panneaux d'OSB permit de mettre en évidence un mode de rupture par perforation des plaques. L'ajout de rondelles permet de limiter ce phénomène. Des connections par pointes lisses, renforcées ou non par des rondelles, connectant un panneau d'OSB avec une poutre en bois furent testées en cisaillement sous chargement monotone et cyclique. L'influence des connections renforcées sur les performances statiques et dynamiques de murs contreventés par des panneaux d'OSB et incluant une très grande ouverture est évaluée expérimentalement. Les combinaisons des paramètres tels que le nombre de tirants d'ancrage, la forme des panneaux, la distribution des clous ainsi que le rajout d'une poutre diagonale furent étudiées. La comparaison de l'énergie dissipée par cycle révéla une meilleure capacité pour les murs renforcés. Les simulations numériques des tests effectués sur les murs sont présentées (essais monotones et cycliques).

Mots clés : éléments finis, ossature bois, contreventement, connexions, énergie dissipée.

Introduction

Light-frame residential construction with properly designed wood-based shear walls has generally performed well in past earthquakes. In the 1995 Kobe earthquake, for example, such buildings survived high seismic forces with little damage. Some bigger multistorey buildings with large openings and irregular plan layouts, however, did not perform adequately. As a result, researchers have been prompted to further examine the performance of shear walls under extreme seismic loading.

Many light-frame shear wall systems have been tested under monotonic loading to determine their ultimate load-carrying capacity (Tissel and Elliott 1977; Council of Forest

Received 19 February 2001. Revised manuscript accepted 3 June 2002. Published on the NRC Research Press Web site at http://cjce.nrc.ca on 17 September 2002.

N. Richard. Laboratoire de mécanique et technologie, 61, avenue du Pt Wilson, 94235 Cachan CEDEX, France.
L. Daudeville.[1] Laboratoire sols solides structures, Domaine Universitaire, B.P. 53, 38041 Grenoble CEDEX 9, France.
H. Prion and F. Lam. Department of Wood Science, The University of British Columbia, 4041-2424 Main Mall, Vancouver, BC V6T 1Z4, Canada.

Written discussion of this article is welcomed and will be received by the Editor until 28 February 2003.

[1]Corresponding author (e-mail: Laurent.Daudeville@inpg.fr).

 DOI: 10.1139/L02-050

Industries of British Columbia 1979; Atherton 1983; Adams 1987; Lam et al. 1997). Other studies involving tests of full-sized shear walls under reversed cyclic loading include those by Rose (1995) and Karacabeyli and Ceccotti (1996). Others also studied the performance of light-frame perforated shear walls under monotonic and reversed cyclic lateral loads (Johnson and Dolan 1996; He et al. 1999).

Further insight into the seismic behaviour of these systems was sought under pseudodynamic (Kamiya et al. 1996) and dynamic (Stewart 1987; Dolan 1989; Durham et al. 1998) loading. Results from some of these tests were used to verify analytical models designed to predict the response of shear walls to given seismic input. For example, Dolan (1989), Filiatrault (1990), and Folz and Filiatrault (2001) constructed models around the hysteretic behaviour of the panel to frame nail connections, which built on and moved forward from linear and nonlinear finite element models developed to predict the load–deformation response of shear walls to monotonic lateral racking loads. These include models by Foschi (1977), Tuomi and McCutcheon (1978), Easley et al. (1982), Itani and Cheung (1984), and Gupta and Kuo (1985).

It is well recognised that the hysteretic behaviour of the panel to frame connectors is central to the lateral response of timber shear walls, thus connector behaviour has been the focus of several studies such as those by Wilkinson (1972), Foschi (1974), Ehlbeck (1979), Hunt and Bryant (1990), and Karacabeyli (1996). Others have used the approach of considering the hysteretic behaviour of entire wall systems to model and predict the dynamic response.

Of particular interest for wood frame structures are cases where large openings severely weaken the walls and potentially cause soft-storey failures. This is very common, for example, for small businesses on narrow building lots with large storefront windows. Whereas much experimental research has been done on conventional shear walls, both statically and dynamically, little information is available on walls that are configured to resemble a portal frame around a large opening.

This paper presents tests results on the static monotonic and cyclic performance of perforated, wood-based shear wall systems and numerical comparisons from a nonlinear finite element program (the dynamic option of the program is not considered in this study). The paper also addresses the influence of reinforcement detailing such as washer-reinforced nailing, the number of hold-downs, the shape of oriented strand board (OSB) panels, the nail distribution, and bracing systems on the shear wall performance.

A description is given of the finite element model developed at Laboratoire de mécanique et technologie (LMT), Cachan, France (Daudeville et al. 1998; Richard et al. 1998). The program is aimed at the analysis of wood structures such as walls but also for timber light-frame buildings. The numerical model is only presented in the context of analysing planar wall systems. Such a numerical model may ensure more reliable and economical designs and reduce the number of experimental tests on structural systems, such as shear walls, that are now necessary for the evaluation of their seismic performance.

Of particular importance in the program is the hysteretic modelling of joints (nails, hold-downs, bolts, etc.). A simple model that takes into account strength degradation is presented. The proposed finite element code is used for the simulation of the presented monotonic and cyclic quasi-static tests. Comparisons between the experimental and predicted results (dissipated energy per cycle, load–displacement curves) are shown to validate the model.

Description of the nailed connections

Connection specimens and wall panel specimens were constructed using kiln-dried nominal 38 × 89 mm number 2 and better spruce–pine–fir dimension lumber and 9.5 mm thick performance-rated W24 OSB panels. All specimens were tested within a few days of manufacturing without further conditioning. Different common nails of lengths 51.0, 63.5, and 76.0 mm with respective shank diameters 3.0, 3.3, and 3.8 mm and head diameters 6.35 (N8), 6.35 (N10), and 7.60 mm (N10) were considered in the study. Common washers with interior and exterior diameters of 5.76 and 11.30 mm were introduced as a means to reinforce the nail connection to represent nails with large heads.

Note that the use of washers prevents overdriven nails and pull-through failure but is not compatible with common construction practice. Recent work has focused on adding a thin metallic strap around the sheathing that gives a washer-like reinforcement but enables pneumatically driven nails.

Hysteretic modelling of the connections

A common observation from tests performed on wood-frame structural systems is that the hysteretic behaviour of the system is governed by the hysteretic behaviour of its primary connections (Dolan 1989; Foliente 1995). Therefore, the behaviour of nailed sheathing governs the response of shear walls under lateral loads. Some of the results of tests performed on the primary connections are presented and, based on the characteristics of the cyclic response of the connector, a hysteretic model of the wood joint is proposed that takes into account the degrading response of the connection under cyclic loading.

Monotonic tests on connections

Shear tests on single-lap sheathing-to-framing connections were performed with the 51 and 76 mm common nails, with and without washers. At each test only one nail was tested, and the edge distance was 75 mm. The load–slip curves of nail connections with or without washer reinforcement are shown in Figs. 1–3. The main differences between the curves concern the maximum load, the corresponding displacement, and the post-peak behaviour. For both lengths, nails without washer reinforcement generally exhibited a more severe load reduction in the post-peak region as a result of pull-through-type failures. Nails with washer reinforcement exhibited more ductile behaviour due to the deformation of the wood caused by the nail shank reacting against the framing member. Eventually this led to a pullout-type failure. Depending on the density of the framing member and the OSB, some pull-through failures also took place, resulting once again in brittle failure. The monotonic load–slip response of the nail connections with washer reinforcement also tends to be less variable compared with that of nail connections without washer reinforcements. Figure 1

Fig. 1. Lateral force – displacement response of the 76 mm nail connections with no washers (*a*) and with washers (*b*).

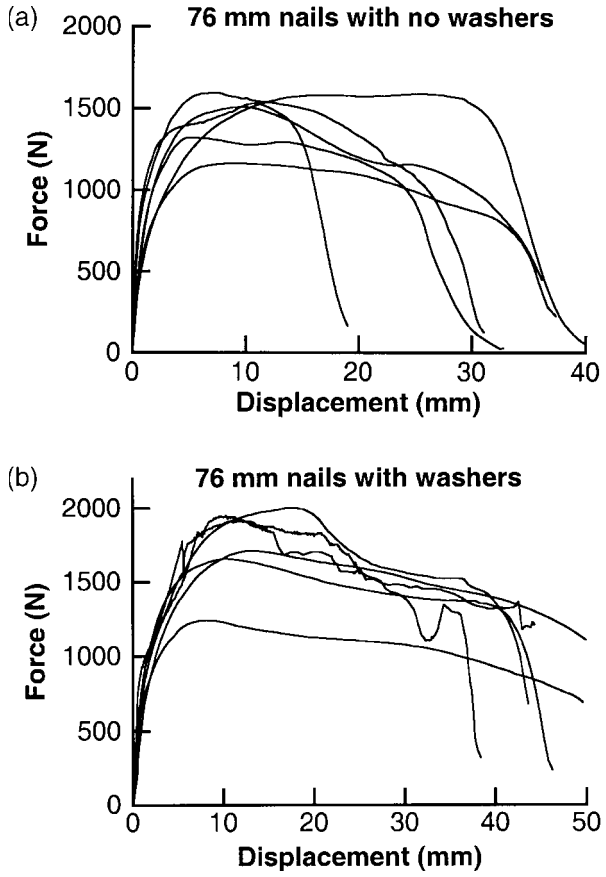

Fig. 2. Lateral force – displacement responses of the 51 mm nail connections with no washers (*a*) and with washers (*b*) under cyclic loading.

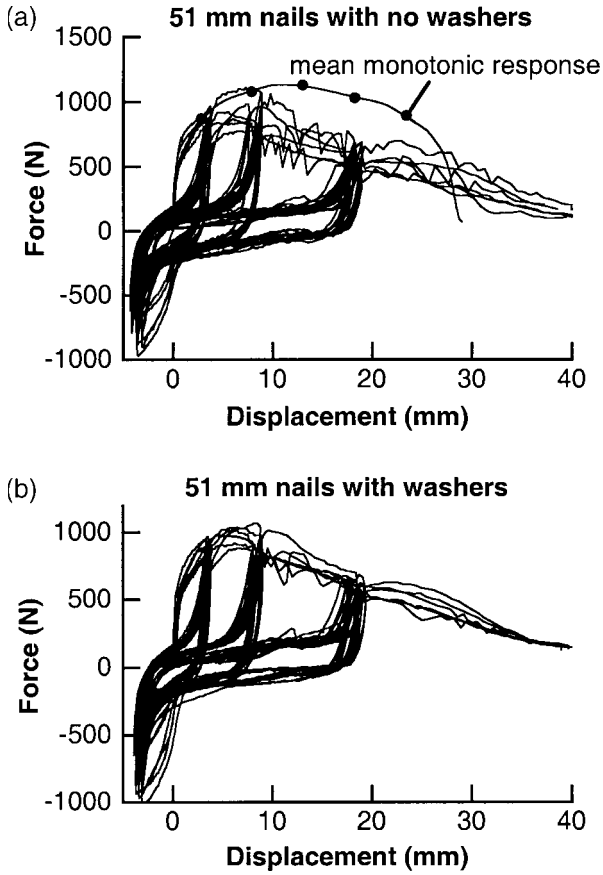

represents the different responses of the 76 mm nails with and without washers. Similar behaviour was observed with the 51 mm nails.

Cyclic tests on connections

Cyclic tests on nailed connections were performed using a modified load schedule based on a protocol originally proposed by He et al. (1998). This load schedule consists of the following sequence: (*i*) three cycles to the displacement at 80% of peak load obtained from a monotonic test, (*ii*) three cycles to the displacement at peak load, (*iii*) three cycles to twice the displacement at peak load, and (*iv*) a final ramp until failure. Each cycle was applied at a frequency of 0.009 Hz. This severe protocol will cause extensive inelastic behaviour at the connections. This mobilizes the energy-dissipating characteristics of the connection without causing fatigue fractures in the nails, as observed in many other tests with long loading protocols (ASTM 1993; Dolan 1994), whereas such a failure mode was not observed in buildings subjected to earthquakes or during dynamic tests on shear walls (He et al. 1998). This modified procedure also has an asymmetric displacement to force the specimen failure in one direction due to the withdrawal or pull-through of the nail.

As shown in Fig. 2, there is no detectable difference in the cyclic response of the 51 mm nail connection with or without washer reinforcement. For the 76 mm nail connection (Fig. 3), however, the post-peak cyclic response is improved with reinforcement. This observation is different from the findings of the monotonic tests where significant improvement in post-peak response can be observed in both the 51 mm and 76 mm washer-reinforced nail connections (Fig. 1). The failure mechanism of the 51 mm washer-reinforced nail connection in the cyclic tests is also quite different from that in the static test. Here, all the specimens failed in pullout mode.

Since the cyclic response of the shorter unreinforced 51 mm nail connection is governed by pullout mode; washer reinforcement cannot improve its cyclic performance. The longer 76 mm nail connections have better anchorage, however, and therefore all the unreinforced 76 mm nail specimens failed in pull-through (one could not even sustain the last set of cycles) and washer reinforcement significantly improved their post-peak cyclic performance. Furthermore, the post-peak response of the reinforced 76 mm nail connection seems to be very repeatable.

Connection model

The proposed model for dowel-type fasteners (bolts, nails, etc.) considers the nonlinear relationship between the laterally applied force F and the connection slip Δ of the constitutive wooden elements (framing and (or) sheathing). It is a phenomenological approach which assumes that the relative drift direction varies weakly during the loading history.

Fig. 3. Lateral force – displacement responses of the 76 mm nail connections with no washers (*a*) and with washers (*b*) under cyclic loading.

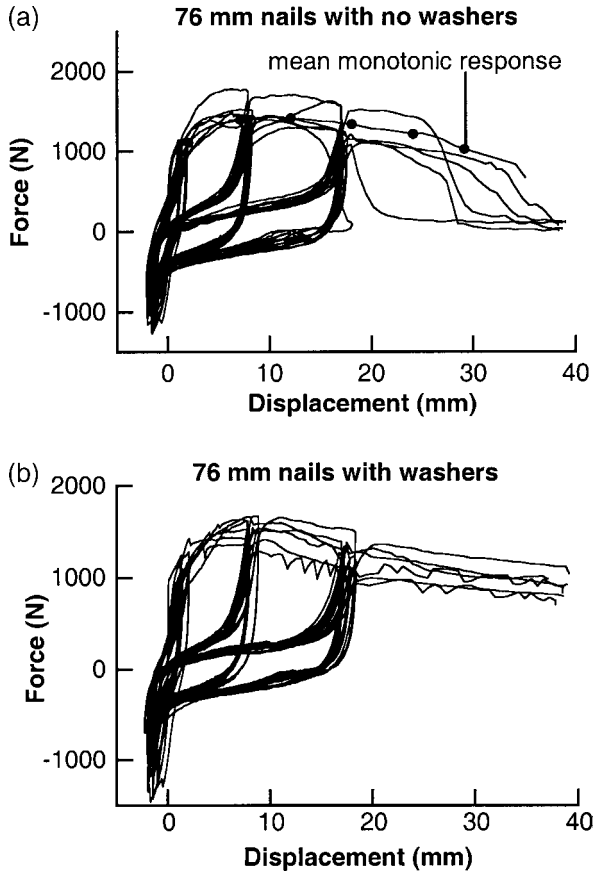

The global nonlinear behaviour of a connection (nail type) is a result of the following phenomena: crushing of the surrounding wood, formation of a plastic hinge in the shank of the nail, friction between nail and wood, and crushing by the nail's head. Previous experimental studies have shown that the behaviour of the nails is not very dependent on the orientation of the wood fibre (for instance, with plywood) (Sieber et al. 1997), therefore the load-direction effects are ignored in the model for nailed connections. Based on these two assumptions, uniaxial tests on connections are sufficient to determine the parameters for the model.

The following functions are proposed to model the uniaxial load–slip behaviour under monotonic loading (Fig. 4). First, an exponential relationship F_1 (Foschi 1974) is used, followed by a linear post-peak softening branch F_2 (Dolan 1989), a second linear softening branch F_3, and a final cutoff F_4 (corresponding to the failure):

$$[1] \qquad F_1(\Delta) = (P_0 + K_1\Delta)\left[1 - \exp\left(-\frac{K_0\Delta}{P_0}\right)\right] \qquad \text{with } 0 \le \Delta \le D_1$$

$$[2] \qquad F_2(\Delta) = F_1(D_1) + K_2(\Delta - D_1) \qquad \text{with } D_1 \le \Delta \le D_2$$

Fig. 4. Proposed force–displacement model for the nailed connections.

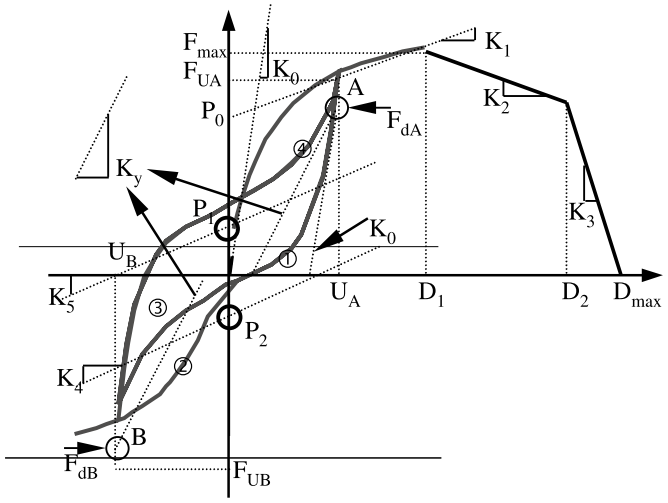

$$[3] \qquad F_3(\Delta) = F_2(D_2) + K_3(\Delta - D_2) \qquad \text{with } D_2 \le \Delta \le D_{\max}$$

$$[4] \qquad F_4(\Delta) = 0 \qquad \text{with } \Delta > D_{\max}$$

With reference to Fig. 4, A denotes the first loading side and B the opposite side. The adopted sign convention is as follows: Δ and F are positive on the A side and negative on the B side. Equations [1]–[4] are presented for the A side. For the B side, one should change the sign of $F(\Delta)$ and put $|\Delta|$ instead of Δ in the equations. Eight parameters as identified in Fig. 4 are required for the complete monotonic loading model: equivalent elasticity limit P_0, elastic modulus K_0, plastic modulus K_1, first softening modulus K_2, second softening modulus K_3, displacement at maximum strength D_1, ultimate displacement D_2, and zero force displacement $D_{\max}$.

Only one linear softening branch (K_2) and a cutoff are often sufficient to describe the monotonic curve of a nailed joint. Nevertheless, a more general model with a second linear softening branch (K_3) is adopted to describe the possible response of other types of connections. The term K_2 can be negative (most usual case) or positive (when the relationship is more ductile).

The cyclic loading rules are based on the four exponential hysteretic curves proposed by Dolan (1989) to describe the pinching behaviour and modified to take into account damage under cyclic loading:

$$[5] \qquad F(\Delta) = F_{dA} + (K_4\Delta + P_2 - F_{dA}) \times \left\{1 - \exp\left[\frac{K_0(U_A - \Delta)}{2P_2}\right]\right\} \qquad \text{branch 1}$$

$$[6] \qquad F(\Delta) = F_{dB} + (K_4\Delta + P_2 - F_{dB}) \times \left\{1 - \exp\left[-\frac{K_y(U_B - \Delta)}{2P_2}\right]\right\} \qquad \text{branch 2}$$

Table 1. Model parameters from six cyclic tests for each group of nails.

Parameter	Short nails (51 mm)	Medium nails (63.5 mm)	Long nails (76 mm) plus washers
D_1 (10^{-3} m)	10	10	10
D_2 (10^{-3} m)	35	35	35
D_{max} (10^{-3} m)	37	37	37
K_0 (10^3 N/m)	900	1200	1300
K_1 (10^3 N/m)	30	35	37
K_2 (10^3 N/m)	–20	–20	–20
K_3 (10^3 N/m)	–900	–900	–900
P_0 (N)	850	1100	1250
P_1 (N)	300	300	300
P_2 (N)	–250	–250	–250
k	0.02	0.02	0.02
γ	0.45	0.45	0.45
D_y (10^{-3} m)	1.5	1.5	1.5

[7] $$F(\Delta) = F_{dB} + (K_5\Delta + P_1 - F_{dB}) \times \left\{1 - \exp\left[\frac{K_0(U_B - \Delta)}{2P_1}\right]\right\} \quad \text{branch 3}$$

[8] $$F(\Delta) = F_{dA} + (K_5\Delta + P_1 - F_{dA}) \times \left\{1 - \exp\left[-\frac{K_y(U_A - \Delta)}{2P_1}\right]\right\} \quad \text{branch 4}$$

where $K_4 = \frac{P_2}{U_A}$, $K_5 = \frac{P_1}{U_B}$, and $K_y = \frac{F(D_y)}{D_y}$; D_y is the yield displacement that is determined from experiments (Yasumura and Kawai 1997) and $F(D_y)$ is the corresponding force (computed with the monotonic loading equation); U_A and U_B are the maximum and minimum slip, respectively, reached during the previous loading history; K_y is the after-degradation stiffness; and K_4 and K_5 are the first and second pinching slopes, respectively.

It is assumed that the second cycle strength degradation on one side (determination of F_{dA} and F_{dB}, respectively) is proportional to the maximum load reached on the other side (F_{U_B} and F_{U_A}, respectively) corresponding to U_B and U_A, respectively:

[9] $$F_{dA} = F_{U_A} - \alpha_A[F_{U_A} - (P_1 + K_5U_A)]$$

with

$$\alpha_A = k\left|\frac{F_{U_B}}{F_{max}}\right|$$

[10] $$F_{dB} = F_{U_B} - \alpha_B[F_{U_B} - (P_2 + K_4U_B)]$$

with

$$\alpha_B = k\left|\frac{F_{U_A}}{F_{max}}\right|$$

Fig. 5. Comparison between cyclic test and model for a 51 mm nail with no washer.

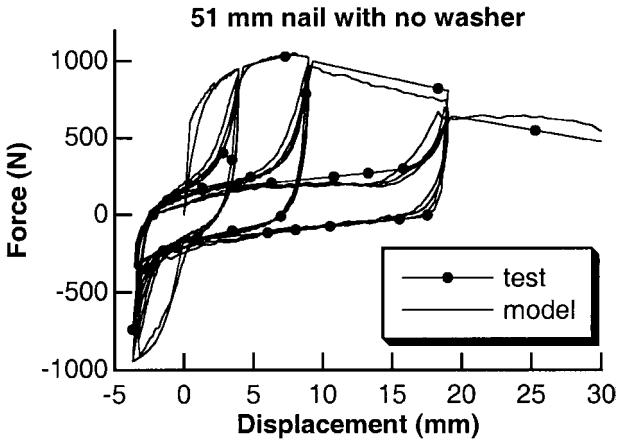

Fig. 6. Example of a shear wall test.

The envelope curve is modified to take into account the degradation of strength due to the withdrawal of the nail outside its hole. The post-peak monotonic strength ($|\Delta| > D_1$) is multiplied by parameters β_A and β_B, respectively:

[11] $$\beta_A = \gamma\left(\frac{U_A - D_1}{D_{max} - D_1}\right)$$

and

Fig. 7. Details of the walls configurations.

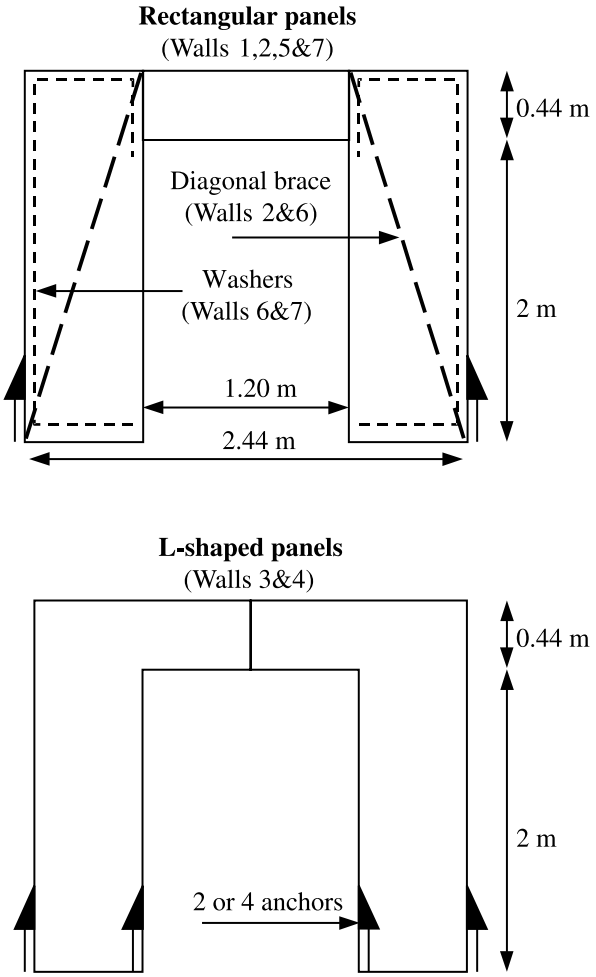

$$\beta_B = \gamma\left(\frac{U_B + D_1}{D_{max} - D_1}\right)$$

There are only five more parameters required for the complete description of the cyclic rules: positive pinching force P_1, negative pinching force P_2, yield displacement D_y, first parameter of degradation k, and second parameter of degradation γ. These can be obtained from the load–slip response curves of the connection (Table 1). A comparison of the experimental and model identified load–slip behaviour of a 51 mm nail connection is shown in Fig. 5.

Shear wall tests

Under monotonic load

Six 2.44 m × 2.44 m wood frame shear walls, each with a symmetrically located opening (1.2 m wide × 2 m high), were tested under monotonic quasi-static lateral loading at the University of British Columbia Earthquake Laboratory. Each wall specimen was mounted in a test frame on a 3.3 m × 3.3 m shake table (Fig. 6). The top of the wall was restrained against both in-plane and out-of-plane movements by means of the rigid frame, and the shake table was controlled to move the base of the wall laterally in the direction parallel to the length of the wall. The maximum stroke of the shake table is 150 mm. Various wall configurations (Fig. 7) were tested to evaluate the influence of the number of hold-downs, the panel shape (rectangular or L-shaped), the nailing density, the use of longer nails with washers as reinforcements, and the use of bracing to reinforce the wall (diagonal wood framing attached to corners with steel plate as shown in Fig. 8). Table 2 summarizes the various parameters for each wall.

Fig. 8. Hold-down device and bracing system of wall 2.

Figure 9 shows the test results of full-size shear walls under monotonic loading (for Figs. 10 and 13–17 the racking load is plotted versus the horizontal displacement at the top of the wall). Wall 1 was a conventional system made with rectangular panels without any reinforcements. Typically, failure initiated at the lintel to wall connection where it opened during loading. Comparisons of results from wall 1 (rectangular panels with 150 mm nail spacing) and wall 2 (braced system) indicate that the addition of braces did not improve the initial stiffness of the system but slightly increased the maximum load capacity of the system by 16%. The L-shaped panels (walls 3 and 4) had the highest initial stiffness, but the sheathing was also heavily damaged under high loads (buckled or tension failure). It was judged that this type of wall would not perform favourably under cyclic loading. The results from walls 3 and 4 show that there was very little difference in response between the L-shaped panel system with two hold-downs and that with four hold-downs. Comparing the results from walls 1 and 5 (reduced nail spacing), however, indicates that wall 5 had a higher capacity (+47.3%), but this could not be sustained beyond a dis-

Table 2. Shear wall monotonic test parameters.

Wall	Description	Nail length (mm)	Perimeter nail spacing (mm)*	No. of hold-downs
1	Rectangular panels	63.5	150	2
2	Braced wall with rectangular panels	63.5	150	2
3	L-shaped panels	63.5	150	2
4	L-shaped panels	63.5	150	4
5	Rectangular panels	63.5	50	2
6	Braced wall with rectangular panels	63.5 and 76 + washers	150	2
7	Rectangular panels	63.5 and 76 + washers	150	2

*Spacing of 300 mm for all interior nailing.

Fig. 9. Racking test responses of walls 1–7 (racking load versus displacement at the top of the wall).

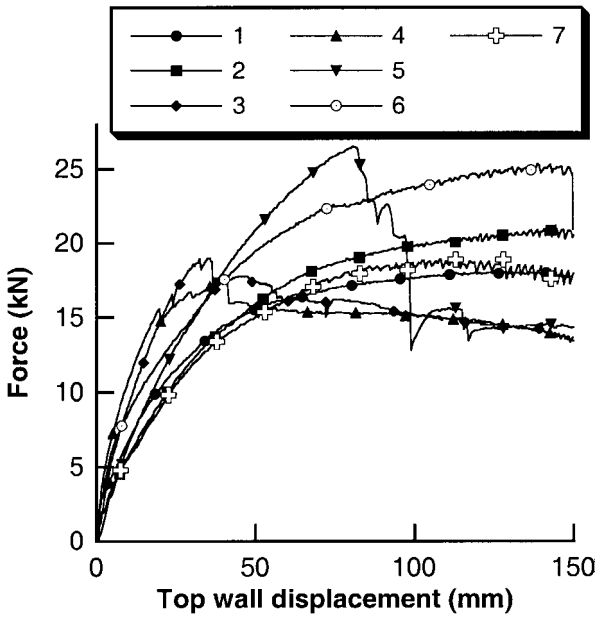

Fig. 10. Monotonic (mono) and cyclic (cycl) force–displacement responses of walls 1 and 7.

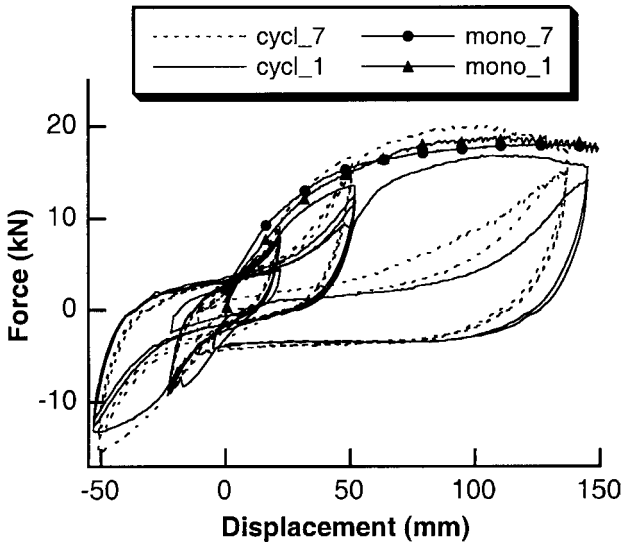

placement of 80 mm because of the failure of one of the hold-downs. This led to uplift of the wall at one corner and the reduced nail spacing no longer governed the behaviour.

The behaviour of a braced wall with rectangular panels and 76 mm nails reinforced with washers was studied in wall 6. This type of reinforcement was only used around the perimeter of the wall specimen, and 63.5 mm long nails were used elsewhere, as shown in Fig. 7. Compared with wall 1, wall 6 had higher stiffness (+60%), higher capacity (+40.6%), and good ductility. A final monotonic test was performed on an unbraced wall with 76 mm washer-reinforced nails (wall 7), and a small increase in maximum load was observed in comparison with wall 1. Some minor construction problems occurred for wall 7 (oblique cutting of some vertical studs, misalignment of the nailing), and as a result a slight decrease in stiffness was observed.

Cyclic tests on shear walls

The configurations of walls 1 and 7 (Table 2) were chosen for two cyclic tests. The construction quality of these two walls, tested under cyclic loading, is identical to that of wall 7, tested under monotonic loading. These two walls, tested under cyclic loading, will be referred to as 1 and 7 in the following part of the paper. The original University of British Columbia protocol (He et al. 1998) was used for these two symmetric cycle tests (three cycles at the corresponding displacement of 50% of the maximum load, then three cycles at 80% of the maximum load, then one cycle back to 50% of the maximum load, and a final pushover). The limit of the shake table was reached for a global displacement of 150 mm.

Comparisons of cyclic versus monotonic responses

The initial stiffnesses are almost identical for the walls of identical construction quality, as shown in Fig. 10. As explained previously, wall 1 presents a higher stiffness under monotonic loading due to its better quality control. Each envelop of the cyclic test response is identical to the envelop of the monotonic test response in terms of maximum load. The post-peak behaviour is slightly different between monotonic and cyclic tests, showing a steeper decline in the load–deformation response for the cyclic tests. These observations on post-peak behaviour are similar to the observations made regarding connections (with and without washers).

Comparisons of the walls with and without washer reinforcements

The main difference between the cyclic response of walls with and without washer reinforcement is the load capacity

Fig. 11. Comparison of the dissipated energy per cycle for wall 1 (nails with no washers) and wall 7 (nails with washers).

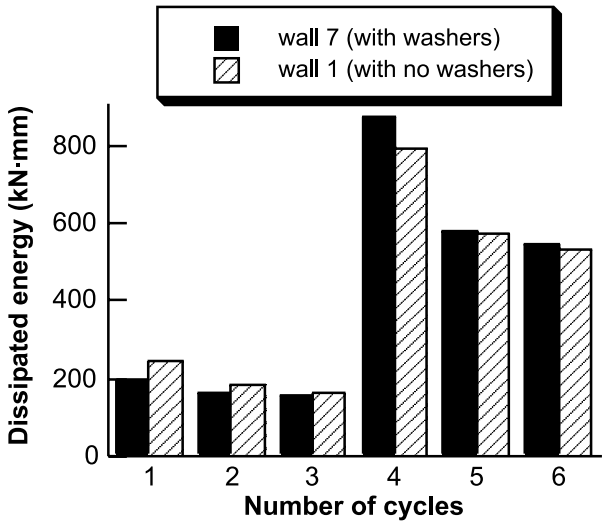

at high displacements. The walls with washer reinforcement were able to sustain much higher loads than the unreinforced walls, despite the failure of some framing members (studs and bottom plates were severely split). The responses to second and third load cycles were also repeatable and stable. In terms of dissipated energy, an average energy drop of 30% was observed between the first and second cycles. The total energy dissipated by the wall (Fig. 11) with and without washer reinforcements is about 5700 and 5400 kN·mm, respectively. Although little difference was observed under cyclic loading between wall 1 and wall 7 in terms of dissipated energy, the advantage of washer-reinforced nailing might be more dominant during the post-peak response, as shown with connection tests, which could show up more prominently in earthquake-based dynamic loading.

Finite element model for shear walls

As mentioned previously, the individual response of a wall is governed by the nonlinear behaviour of its primary connections, as the damage in the structure is essentially localized around the connections. As it is very expensive to test real structures on a seismic shake table, numerical tools capable of representing the nonlinear connection behaviour are essential to further the understanding of the behaviour of wood frame structures under seismic loading. A two-dimensional version of such a numerical model is presented in this paper and is validated against the previously reported test results.

Framing and sheathing

The structural frame is modelled with two-node elastic beam elements, and the sheathing is modelled with four-node elastic orthotropic plate elements.

Framing–sheathing connections

Considering the number of connectors in a single wall or in a larger structure like a building, it is to difficult to model every nailed connection by means of a nonlinear spring con-

Fig. 12. Example of a separation at one corner of the wall.

necting two nodes with the same coordinates. Thus, at each time step of the calculation, the reaction forces at each connection are calculated from the relative displacement between the constitutive elements and transformed to nodal forces applied to the framing and sheathing elements via their shape functions. Note that coupling terms due to the stiffness of the connections appear in the global stiffness matrix. This condensation procedure helps to decrease the global number of degrees of freedom. Dolan (1989) used an identical approach, which was then modified by White (1995). The constitutive behaviour of these nailed connections was presented earlier in the paper.

Framing connections

Two kinds of framing connections, the beam-to-beam and the hold-down, influence the global response of the walls, especially those with openings.

Beam-to-beam connections

Vertical and horizontal framing members are connected together with 90 mm long nails. This is a relatively weak connection. During the wall tests, progressive separation of vertical and horizontal beams in different locations of the structure was observed, as shown in Fig. 12. Tension tests have been conducted on such connections (parallel to the nails) to obtain the corresponding load–slip curve. A bilinear (brittle) model in tension (pull out of the nails) associated with a large stiffness in compression (unilateral contact) is sufficient to approximate the real situation. Under cyclic loading, the secant stiffness is adopted (unloading toward the origin, and reloading on the same straight line). The peak load and the two stiffness terms are necessary to fully describe the load–slip curve. The rotational resistance of this kind of connection is very weak, and consequently it is modelled with a perfect hinge.

Table 3. Model parameters for the hold-down and the beam-to-beam connections.

Parameter	Hold-down	Beam-to-beam
D_1 (10^{-3} m)	10	1.3
D_2 (10^{-3} m)	11	—
D_{max} (10^{-3} m)	12	14.6
K_0 (10^3 N/m)	9 000	—
K_1 (10^3 N/m)	1 000	30
K_2 (10^3 N/m)	100	—
K_3 (10^3 N/m)	–10 000	–3
P_0 (N)	1.5×10^6	0

Hold-down connections

On each side of the wall, and sometimes at the bottom of an opening, hold-down connections are used to fix the structure to the concrete foundation (i.e., reaction frame or seismic table). The anchoring systems are placed at a certain distance from the bottom with four bolts. The hold-down devices are typical of those used in Japan (Fig. 8), and they reduce stress concentrations at the corner of the bottom plate. During lateral loading, uplift of the bottom plate may occur. This connection is modelled with an element that links a fixed node (located on the ground) and the node of the corresponding vertical beam. The horizontal and rotary movements are free. The vertical slip obeys a nonlinear law in tension similar to that used for the nail connection (with different parameters). In compression, a strong stiffness is taken to model the unilateral contact of the horizontal beam on the floor. The cyclic rules are simpler than those adopted in the nail connection, since there is only one side of the loading. P_1 and P_2 are equal to zero (and thus K_4 and K_5 remain equal to zero), and there is no strength degradation when cycling.

The constitutive behaviours of the two previous connections were identified from tests performed on individual connections, and the parameters are given in Table 3.

Note that the contact between two sheathing plates was not modelled because its influence can be neglected (Richard 2001). The bottom plate uplifted on one side of the wall, but no significant crushing was noticed on the other side of the wall during the tests.

Simulation of monotonic tests

The main parameters of the test structure and the model are as follows: number of nails, presence of washer as a possible reinforcement, nail size, brace system, shape of the sheathing plates, and number of hold-downs. Four modelling approaches were considered and compared against the test results.

(1) The first load–deformation response curves shown in Fig. 13 were obtained when all the sill plates of the node were fixed to the ground. In this situation the hold-downs were not modelled. Beam-to-beam connections were considered as perfect hinges. This modelling approach is not very accurate, and the initial stiffness and the maximum load were not accurately predicted.

Fig. 13. Simulation I versus test results: only the nonlinear behaviour of the nails is considered.

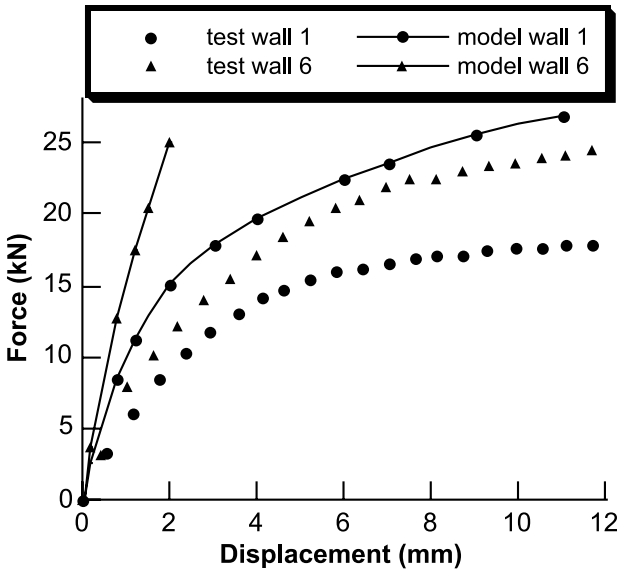

Fig. 14. Simulation II versus test results: nonlinear behaviour of nails and hold-downs are considered.

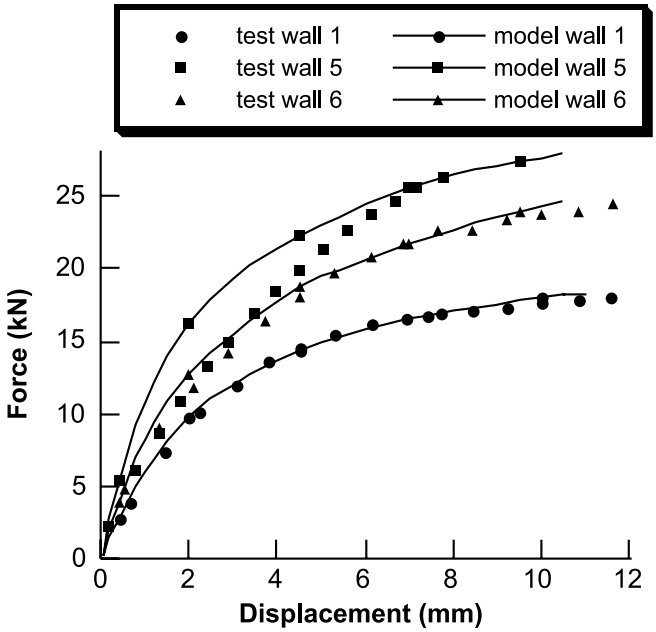

(2) Releasing some beam-to-beam connections on the tension side can improve the fit to the experimental curves; however, this solution is not really robust because it cannot account for the cyclic load case.

(3) In Fig. 14 the hold-down is modelled while beam-to-beam connections remain perfectly elastic. This modification gives good results in terms of initial stiffness and maximum load. Only the hold-down in tension is modelled for the curves; the other hold-down is simply fixed to the ground.

(4) Figure 15 shows the last modelling approach in terms of initial stiffness for four different walls using a bilinear model for the beam-to-beam connections. All connec-

Fig. 15. Simulation III versus test results: all the connections exhibit nonlinear behaviour.

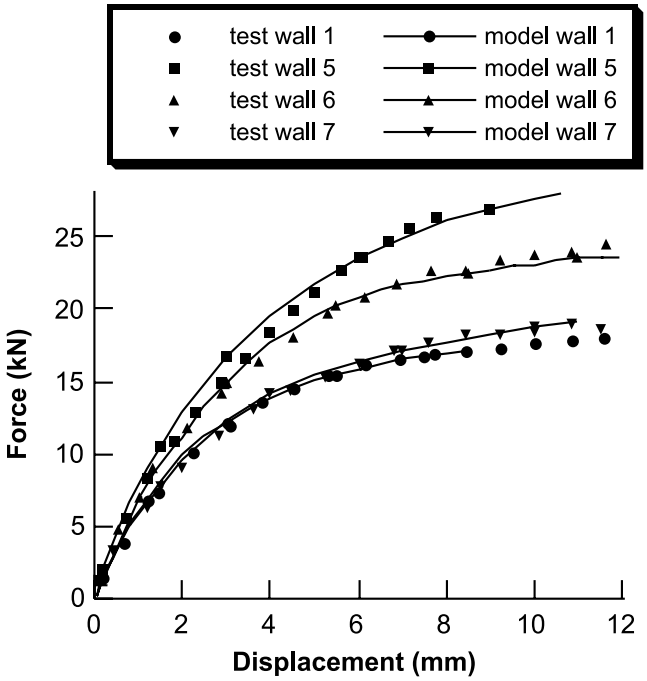

tions inside the structure, including the two hold-downs, were modelled. The model for wall 6, in which metallic joints are used to connect the brace beam to the adjacent beams, includes a plastic hinge for the nodes.

Only three plate elements are required for the model. About 200 nails (an average over the four walls in Fig. 15, including the wall with a reduced nail spacing) were necessary to connect the framing and sheathing members and were modelled.

The need to model all the connections in a structure is clearly shown by the differences between the model and test results (Figs. 13–15). The global nonlinear behaviour is due to all the nonlinearities of the connections. In the case of wood shear walls with a large opening, modelling the nonlinearities of the connections reduces the constraints on the structure which can otherwise lead to unrealistic stiffness and maximum load predictions.

Simulation of the cyclic tests

All the connections are modelled, and it is therefore possible to compare the accuracy of the model results with the results of two cyclic tests performed at the University of British Columbia. Figures 16 and 17 show the comparisons between model and test results for walls 1 and 7. The model precisely predicts the envelope curves defined by the cyclic procedure and the hysteretic curves. Stiffness degradation between the first and second or third cycles is well calculated, proof that constitutive behaviours used for connectors and hold-downs are sufficient to fully describe the response of the global structure. In terms of dissipated energy, Fig. 18 presents results obtained from the tests and the model. In Table 4, test results and model simulation of dissipated energy between two consecutive cycles are compared. Figure 18

Fig. 16. Simulation versus test results: force–displacement curves for wall 1.

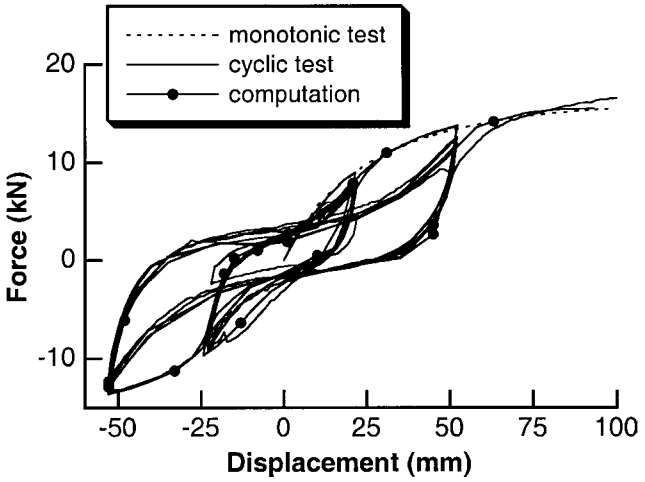

Fig. 17. Simulation versus test results: force–displacement curves for wall 7.

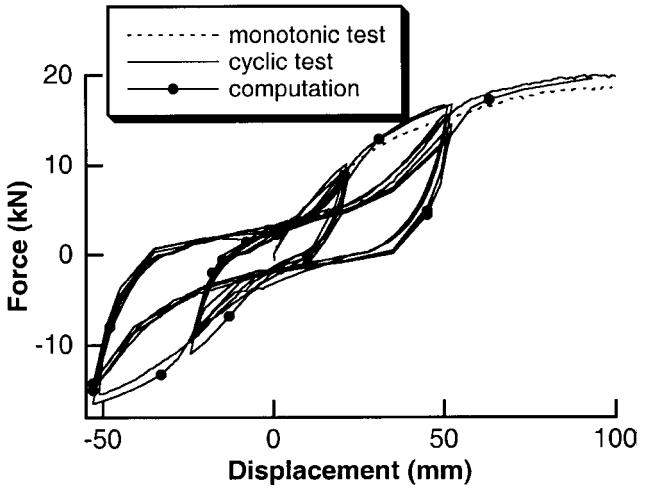

Fig. 18. Simulation versus test results: dissipated energy per cycle for walls 1 and 7.

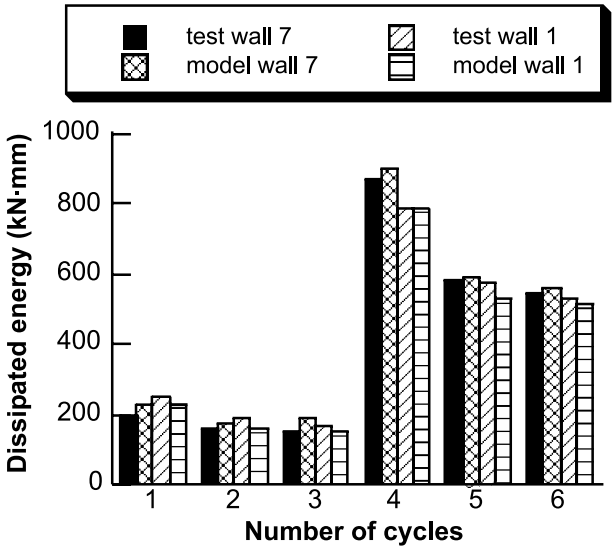

Table 4. Comparison of test results and model simulation of dissipated energy between two consecutive cycles in the two first sets of three cycles.

Wall 1		Wall 7	
Test (%)	Model (%)	Test (%)	Model (%)
First set of three cycles			
75	70	83	75
90	92	95	104
Second set of three cycles			
73	67	67	66
92	96	93	94

Note: The values in the table are the ratios of dissipated energy between the second and the first cycle (first line) and between the third and the second cycle (second line).

and Table 4 show that the dissipated energy and the energy variation from one cycle to another are well predicted.

The simulation of wall 1 test used 162 degrees of freedom to study 141 connections. It took less than 1 min for the monotonic test and about 4 min for the cyclic test on a 233 MHz Pentium II computer.

Conclusions

The experimental part of this project conducted at the University of British Columbia was to study the influence of local reinforcements on the shear response of walls with large openings. Tests on connections were carried out for the material parameter identification of the hysteretic model implemented in the finite element code presented. Reinforcements that were studied included the use of washers, an increased nailing density, a diagonal brace, L-shaped panels instead of regular panels, and hold-downs.

Results for different nail lengths show that the washer reinforcement was not effective for shorter nails (51 mm) under cyclic load but was a significant improvement for longer nails (76 mm). The improvement effect of the washers took place relatively late in the load–slip curve. The longer 76 mm nails were able to provide better anchorage, thus taking advantage of the washer reinforcements. When applied to a shear wall structure, very little improvement for both monotonic and cyclic loading was evident; however, under numerous load cycles, the washers significantly increased the dissipated energy. Walls reinforced with washers dissipated 50% more energy than normal walls.

Parameters such as the number of hold-downs or the shape of the OSB panels improved the initial stiffness but led to sudden failures as the panels were torn or buckled. No cyclic or dynamic tests were conducted on these types of walls. A higher nail density helped to increase the shear capacity, but that system also failed in a brittle mode due to hold-down failures. The best combination seems to be the use of a bracing member with perimeter washer-reinforced 76 mm nails; both initial stiffness and strength were improved.

A finite element model was also presented in the paper. This deterministic approach is applicable because of the large number of nails attaching the sheathing to the framing. The mean response of large populations is statistically valuable (central limit theorem), but the variability of the nail behaviour is low (Figs. 2–3). The comparison of numerical and experimental results showed that this approach is sufficient to accurately predict the behaviour of the shear wall under both monotonic and cyclic loads. A very low computation time is obtained because of the reduced number of degrees of freedom due to the condensation method used.

This numerical tool allows future parametric studies of nail length, nail location in the structure, presence of a brace system, or global design of the wall. This nonlinear dynamic computer analysis program allows the prediction of the dynamic response of wooden structures made of shear walls and diaphragms, and the results are presented in Richard (2001).

References

Adams, N.R. 1987. Plywood shear walls. Research Report 105, American Plywood Association, Tacoma, Wash.

ASTM. 1993. Proposed standard test method for dynamic properties of connections assembled with mechanical fasteners. American Society for Testing and Materials, Philadelphia, Pa.

Atherton, G.H. 1983. Ultimate strength of particleboard diaphragms. Forest Products Journal, **33**(5): 22–26.

Council of Forest Industries of British Columbia. 1979. Douglas-fir plywood diaphragms. Council of Forest Industries of British Columbia (COFI), Vancouver, B.C.

Daudeville, L., Davenne, L., Richard, N., and Kawai, N. 1998. Étude du comportement parasismique de structures à ossature en bois. Revue Française de Génie Civil, **2**(6): 651–665.

Dolan, J.D. 1989. The dynamic response of timber shear walls. Ph.D. thesis, The University of British Columbia, Vancouver, B.C.

Dolan, J.D. 1994. Proposed test method for dynamic properties of connections assembled with mechanical fasteners. Journal of Testing and Evaluation, **22**(6): 542–547.

Durham, J., He, M., Lam, F., and Prion, H.G.L. 1998. Seismic resistance of wood shear walls with oversize sheathing panels. Proceedings of the 5th World Conference on Timber Engineering, Montreux-Lausanne, Switzerland, Vol. 1, pp. 396–403.

Easley, J.T., Foomani, M., and Dodds, R.H. 1982. Formulas for wood shear walls. ASCE Journal of Structural Engineering, **108**(11): 2460–2478.

Ehlbeck, J. 1979. Nailed joints in wood structures. Research Report 166, Virginia Polytechnic Institute and State University, Blacksburg, Va.

Filiatrault, A. 1990. Static and dynamic analysis of timber shear walls. Canadian Journal of Civil Engineering, **17**(4): 643–651.

Foliente, G.C. 1995. Hysteresis modeling of wood joints and structural systems. ASCE Journal of Structural Engineering, **121**(6): 1013–1021.

Folz, B., and Filiatrault, A. 2001. Cyclic analysis of wood shear walls. ASCE Journal of Structural Engineering, **127**(4): 433–441.

Foschi, R.O. 1974. Load-slip characteristics of nails. Wood Science, **7**(1): 69–76.

Foschi, R.O. 1977. Analysis of wood diaphragms and trusses. Part I: Diaphragms. Canadian Journal of Civil Engineering, **4**(3): 345–352.

Gupta, A.K., and Kuo, G.P. 1985. Behaviour of wood framed shear walls. ASCE Journal of Structural Engineering, **111**(8): 1722–1733.

He, M., Lam, F., and Prion, H.G.L. 1998. Influence of cyclic test protocols on performance of wood-based shear walls. Canadian Journal of Civil Engineering, **25**: 539–550.

He, M., Magnusson, H., Lam, F., and Prion, H.G.L. 1999. Cyclic performance of perforated wood shear walls with oversized panels. ASCE Journal of Structural Engineering, **125**(1): 10–18.

Hunt, R.D., and Bryant, A.H. 1990. Laterally loaded nail joints in wood. ASCE Journal of Structural Engineering, **116**(1): 111–124.

Itani, R.Y., and Cheung, C.K. 1984. Nonlinear analysis of sheathed wood diaphragms. ASCE Journal of Structural Engineering, **110**(9): 2137–2147.

Johnson, A.C., and Dolan, J.D. 1996. Performance of long shear walls with openings. Proceedings of the International Wood Engineering Conference, New Orleans, La., Vol. 2, pp. 337–344.

Kamiya, F., Sugimote, K., and Mii, N. 1996. Pseudo-dynamic test of sheathed wood walls. Proceedings of the International Wood Engineering Conference, New Orleans, La., Vol. 2, pp. 187–194.

Karacabeyli, E. 1996. Quasi-static reversed-cyclic testing of nailed joints. Proceedings of the 29th CIB-W18 Meeting, Universität Karlsruhe, Karlsruhe, Germany, Paper 29-7-7.

Karacabeyli, E., and Ceccotti, A. 1996. Test results on the lateral resistance of nailed shear walls. Proceedings of the International Wood Engineering Conference, New Orleans, La., Vol. 2, pp. 179–186.

Lam, F., Prion, H.G.L., and He, M. 1997. Lateral resistance of wood shear walls with large sheathing panels. ASCE Journal of Structural Engineering, **123**(12): 1666–1673.

Richard, N. 2001. Approche multi-échelles pour la modélisation des structures bois sous sollicitations sismiques. Doctorat de l'École Normale Supérieure de Cachan, Cachan, France.

Richard, N., Daudeville, L., Davenne, L., and Kawai, N. 1998. Numerical analysis of seismic response of timber shear walls with nailed joints. Proceedings of the 11th European Conference on Earthquake Engineering, Paris.

Rose, J.D. 1995. Performance of wood structural panel shear walls under cyclic (reversed) loading. Proceedings of the 49th Forest Products Society Annual Meeting, Portland, Oreg.

Sieber, D., Lam, F., and Prion, H.G.L. 1997. The behavior of nailed sheathing-to-frame connections under static and cyclic load. Internal report, Department of Wood Science, The University of British Columbia, Vancouver, B.C.

Stewart, W.G. 1987. The seismic design of plywood sheathed shearwalls. Ph.D. thesis, University of Canterbury, Christchurch, New Zealand.

Tissel, J.R., and Elliott, J.R. 1977. Plywood diaphragms. Research Report 138, American Plywood Association, Tacoma, Wash.

Tuomi, R.L., and McCutcheon, W.J. 1978. Racking strength of light-frame nailed walls. ASCE Journal of Structural Engineering, **104**(7): 1131–1140.

White, M. 1995. Parametric study of timber shear walls. Ph.D. thesis, Virginia Polytechnic Institute and State University, Blacksburg, Va.

Wilkinson, T.L. 1972. Analysis of nailed joints with dissimilar members. ASCE Journal of Structural Engineering, **98**(9): 2005–2013.

Yasumura, M., and Kawai, N. 1997. Evaluation of wood framed shear walls subjected to lateral loads. Proceedings of the 30th CIB-W18 Meeting, Universität Karlsruhe, Karlsruhe, Germany, Paper 30-15-4.

List of symbols

D_{max}	zero force displacement
D_y	yield displacement
D_1	displacement at maximum strength
D_2	ultimate displacement
F	laterally applied force
F_d	after-degradation strength
F_{max}	maximum strength
F_{dA}, F_{dB}	after-pinching strength
F_{U_A}, F_{U_B}	maximum strength at slips U_A and U_B
F_1, F_2, F_3, F_4	model functions
k	first parameter of degradation
K_y	after-degradation stiffness
K_0	elastic modulus
K_1	plastic modulus
K_2	first softening modulus
K_3	second softening modulus
K_4	first pinching slope
K_5	second pinching slope
P_0	equivalent elasticity limit
P_1	pinching force (positive)
P_2	pinching force (negative)
U_A	maximum slip
U_B	maximum slip (on the opposite direction of U_A)
α_A, α_B	degradation functions under reversed loading
β_A, β_B	second degradation functions under reversed loading
Δ	connection slip
γ	second parameter of degradation